Redox Biology 75 (2024) 103281

Contents lists available at ScienceDirect

Redox Biology

journal homepage: www.elsevier.com/locate/redox

Therapeutic efficacy of ECs Foxp1 targeting Hif1α-Hk2 glycolysis signal to restrict angiogenesis

Jingjiang Pi [a,b,c,1], Jie Liu [a,1], Huan Chang [d,1], Xiaoli Chen [a,1], Wenqi Pan [a], Qi Zhang [c], Tao Zhuang [a,e], Jiwen Liu [a], Haikun Wang [f], Brian Tomlinson [g], Paul Chan [h], Yu Cheng [i], Zuoren Yu [a], Lin Zhang [a], Zhenlin Zhao [b,*], Zhongmin Liu [a,**], Jie Liu [a,b,***], Yuzhen Zhang [a,****,2]

[a] State Key Laboratory of Cardiovascular Diseases and Medical Innovation Center, Shanghai Heart Failure Research Center, Department of Cardiology, Department of Cardiovascular Surgery, Shanghai East Hospital, Tongji University School of Medicine, Shanghai, 200120, China
[b] Shenzhen Ruipuxun Academy for Stem Cell and Regenerative Medicine, Shenzhen, China
[c] Department of Cardiology, Shanghai East Hospital, Tongji University School of Medicine, Shanghai, 200120, China
[d] Department of Electrophysiology, Jingjiang People's Hospital Affiliated to Yangzhou University, Yangzhou, 225000, China
[e] Department of Physiology and Pathophysiology, School of Basic Medical Sciences, Fudan University, Shanghai, 200032, China
[f] CAS Key Laboratory of Molecular Virology and Immunology, Institut Pasteur of Shanghai, Chinese Academy of Science, University of Chinese Academy of Sciences, 320 Yueyang Rd, Shanghai, 200031, China
[g] Faculty of Medicine, Macau University of Science and Technology, Macau SAR, China
[h] Division of Cardiology, Department of Internal Medicine, Wan Fang Hospital, Taipei Medical University, Taipei, Taiwan
[i] Institute for Biomedical Engineering and Nano Science, Tongji University School of Medicine, Shanghai, China

ARTICLE INFO

Keywords:
Transcription factor Foxp1
Angiogenesis
Xenograft tumor
Endothelial cells
Glycolysis

ABSTRACT

Endothelial cells (ECs) rely on glycolysis for energy production to maintain vascular homeostasis and the normalization of hyperglycolysis in tumor vessels has recently gained attention as a therapeutic target. We analyzed the TCGA database and found reduced Foxp1 expression in lung carcinoma. Immunostaining demonstrated reduced expression more restricted at tumor vascular ECs. Therefore, we investigated the function and mechanisms of Foxp1 in EC metabolism for tumor angiogenesis required for tumor growth. EC-Foxp1 deletion mice exhibited a significant increase of tumor and retinal developmental angiogenesis and Hif1α was identified as Foxp1 target gene, and Hk2 as Hif1α target gene. The Foxp1-Hif1α-Hk2 pathway in ECs is important in the regulation of glycolytic metabolism to govern tumor angiogenesis. Finally, we used genetic deletion of EC-Hif1α and RGD-peptide nanoparticles EC target delivery of Hif1α/Hk2-siRNAs to knockdown gene expression which reduced the tumor EC hyperglycolysis state and restricted angiogenesis for tumor growth. This study advances our understanding of EC metabolism for tumor angiogenesis, and meanwhile provides evidence for future therapeutic intervention of hyperglycolysis in tumor ECs for suppression of tumor growth.

* Corresponding authors.
** Corresponding author. Research Center for Translational Medicine, Shanghai Heart Failure Research Center, Department of Cardiovascular Surgery, Shanghai East Hospital, Tongji University School of Medicine, 150 Jimo Rd, Pudong New District, Shanghai, 200120, China.
*** Corresponding authors. Key Laboratory of Arrhythmias of the Ministry of Education of China, Research Center for Translational Medicine, Shanghai Heart Failure Research Center, Shanghai East Hospital, Tongji University School of Medicine, 150 Jimo Rd, Pudong New District, Shanghai, 200120, China.
**** Corresponding author. Key Laboratory of Arrhythmias of the Ministry of Education of China, Research Center for Translational Medicine, Shanghai Heart Failure Research Center, Shanghai East Hospital, Tongji University School of Medicine, 150 Jimo Rd, Pudong New District, Shanghai, 200120, China.
E-mail addresses: 1012pjj@tongji.edu.cn (J. Pi), pjj1012@126.com (Z. Zhao), liu.zhongmin@tongji.edu.cn (Z. Liu), kenliujie@126.com (J. Liu), yzzhang-tj@tongji.edu.cn (Y. Zhang).
[1] These authors contributed equally to this work.
[2] Further information and requests for resources and reagents should be directed to and will be fulfilled by the lead contact, Yuzhen Zhang (yzzhang-tj@tongji.edu.cn)

https://doi.org/10.1016/j.redox.2024.103281
Received 25 May 2024; Received in revised form 21 July 2024; Accepted 21 July 2024
Available online 26 July 2024

1. Introduction

Endothelial cells (ECs) form the inner lining of blood vessels and are essential for the normal function of the vascular system. The vascular network expands in response to changing metabolic demands during physiological embryonic development, organ growth or pathological tumor growth to supply tissues with sufficient oxygen and nutrients [1,2]. ECs stay mostly quiescent in physiological conditions; however, they retain the capacity of rapid switch to a highly proliferative and migratory state for initiation of new vessels formation in response to injury or under pathological conditions, a process called sprouting angiogenesis that is tightly regulated [1,2].

Tumor angiogenesis is the critical process required for tumor growth and progression [3]. The newly formed vasculature within a tumor is highly disordered both structurally and functionally, and ECs that comprise tumor vasculature are poorly connected causing vessel leakage and exposing the endothelium to a hypoxic microenvironment, therefore, most anti-angiogenic therapies have limited success and result in

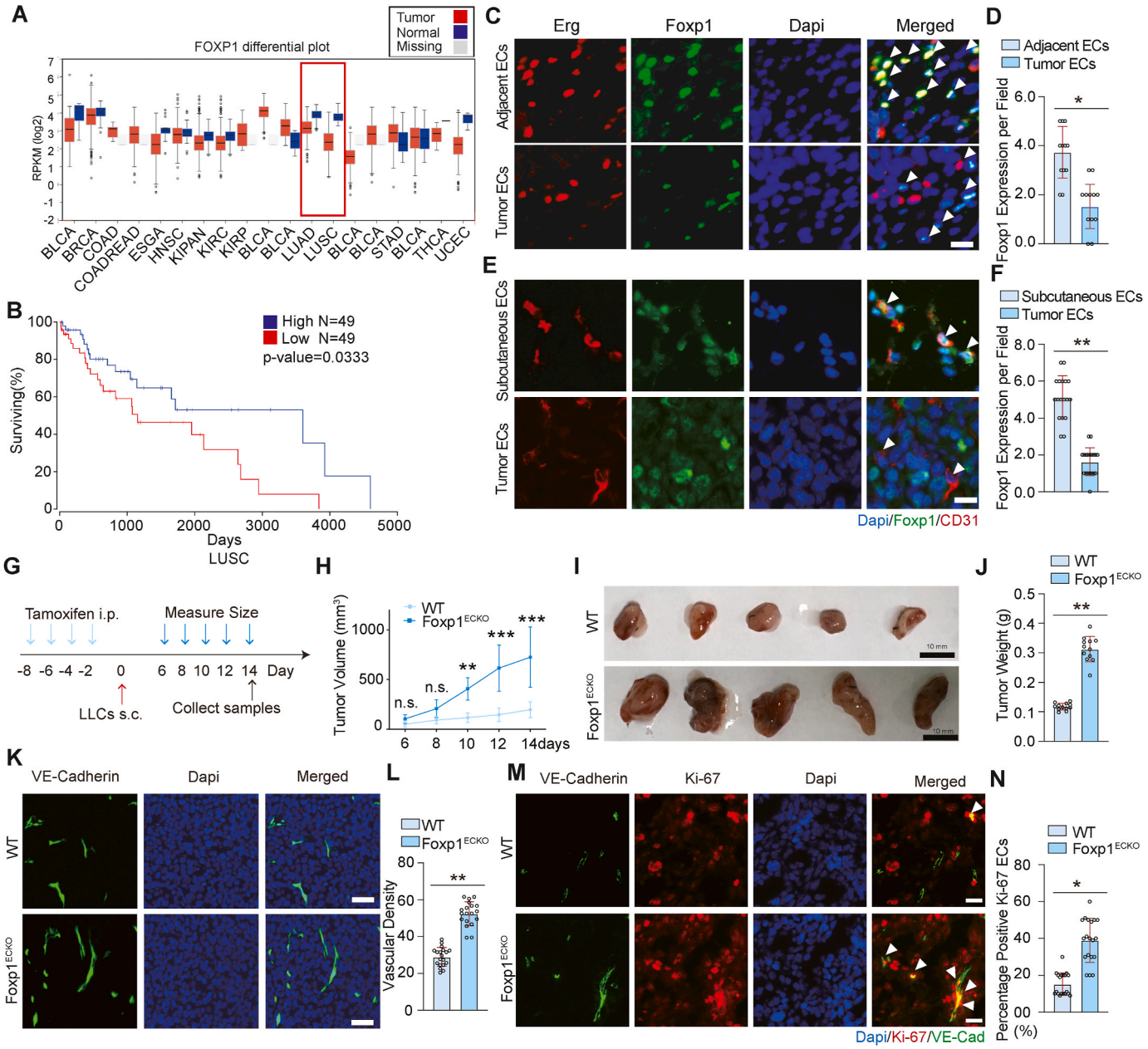

Fig. 1. Reduced Foxp1 expression in lung tumors and endothelial Foxp1 deletion inhibits tumor angiogenesis and suppresses tumor growth. (A) Dataming of TCGA database for Foxp1 expression in lung squamous cell carcinoma (LUSC) and adenocarcinoma (LUAD) compared to adjacent tissues. (B) Analysis of Foxp1 expression level and the survival time of LUSC patients in TCGA database of NIH Cancer Genome Atlas Program. (C–F) The representative images of Foxp1 immunostaining in vascular endothelial cells (ECs) of human LUSC samples from Shanghai Outdo Biotech compared to adjacent normal tissues (C–D), and of mouse LLC xenograft tumor compared to the subcutaneous ECs indicated by white arrow heads (E–F), with quantification data on the right. (G) The schematic chart of tamoxifen administration for induction of EC-Foxp1 deletion in mouse LLC1 xenograft tumor model. (H–J) The LLC1 xenograft tumor growth (H), final tumor size (I) and mass (J) in Foxp1^{ECKO} mutant and littermate wild-type control mice. (K–N) The representative images of tumor vessel density (K–L) and Ki-67 positive ECs marked with arrow heads (M–N) in LLC1 xenograft sections of Foxp1^{ECKO} mutant and wild-type mice, with quantification data on the right. All data were presented as mean ± SEM, and analyzed using standard two-tailed Student's t-test. *, $P < 0.05$; **, $P < 0.01$. Fig. 1L and N quantitative data in accordance with normal distribution. Scale bars: C, E, 50 μm; I, 10 mm; K, 100 μm; M, 50 μm.

acquired resistance to the increased hypoxia due to reduction of the vasculature [2,4]. The metabolism of ECs has only recently been recognized as a driving force of angiogenesis and targeting EC metabolism could prove to be an alternative anti-angiogenic therapy [5,6]. Hence, it is pertinent to know how ECs alter their metabolism during diseases in order to pave the way for novel therapeutic opportunities for pathological angiogenesis, as in cancers.

ECs have a relatively low mitochondrial content and are dependent on glycolysis for energy production [7]. The master regulators of hypoxia response pathway, hypoxia-inducible factors (Hifs), reinforce the glycolytic dependence of ECs under hypoxic conditions and promote ECs angiogenesis through regulation of the expression of proteins that mediate the cellular response to hypoxia [8–10]. However, the metabolic alterations of ECs in response to hypoxia, especially in tumor vasculature, have been relatively unexplored.

Foxp (forkhead box P) factors are large modular transcriptional repressors that bind to DNA via their highly conserved forkhead DNA-binding domain to regulate a large number of genes involved in cell proliferation and differentiation required for normal organ development [11,12]. Foxp1 is the most highly expressed Foxp family-protein in ECs and was reported to stimulate angiogenesis [13], which is in contrast to our finding that EC-Foxp1 deletion resulted in increased xenograft tumor angiogenesis to promote tumor growth. In order to clarify this discrepancy, we searched the TCGA database of the NIH Cancer Genome Atlas Program and found reduced Foxp1 expression in lung squamous cell carcinoma (LUSC) and lung adenocarcinoma (LUAD). Further studies showed reduced Foxp1 expression more specifically in vascular ECs of tumors, such as LUAD of human microarray and Lewis lung carcinoma cell (LLC1) xenograft tumor model. Therefore, we generated EC-Foxp1 loss-of-function and gain-of-function mice to explore the effects and mechanisms of Foxp1 on ECs metabolism that further influence tumor angiogenesis required for tumor growth and progression, in order to gain a deeper understanding of the detailed features and provide novel metabolism-centric therapies of normalizing hyperglycolysis in tumor ECs to suppress tumor growth.

2. Results

2.1. Foxp1 expression is reduced in lung tumor ECs and loss of Foxp1 in ECs increases LLC1 xenograft tumor angiogenesis and promotes tumor growth

Foxp1 is widely expressed in tissues important for development of many organs and can serve as either a tumor suppressor [14,15] or an oncogene [16–18]. We searched the TCGA database of NIH Cancer Genome Atlas Program (http://www.cbioportal.org/) and the analysis showed reduced Foxp1 expression in LUSC and lung adenocarcinoma (LUAD) compared to the tissue adjacent to the tumor (Fig. 1A), and the reduction of Foxp1 expression in tumors was associated with shorter survival time of patients (Fig. 1B). Immunostaining of human LUAD tissue microarray from Shanghai Outdo Biotech (Cat No. HLugA030PG03) showed reduced Foxp1 expression more specifically in tumor ECs (Fig. 1C–D) and the clinical information of LUAD patients were shown in Supplementary Table 1. We further confirmed a significant reduction of Foxp1 expression in ECs of Lewis lung carcinoma cell (LLC1) xenograft tumor compared to the subcutaneous ECs adjacent to the tumor (Fig. 1E–F). These results suggested a possible role of EC-Foxp1 in the regulation of tumor angiogenesis influencing tumor growth and progression.

To determine the *in vivo* effects of EC-Foxp1 on tumor angiogenesis and further tumor growth, we generated EC-specific Foxp1 deletion mice, Foxp1^{ECKO}, and LLC1 xenograft tumor model was used as reported in our previous study [19]. Tamoxifen administration for EC-Foxp1 specific deletion was shown in the schematic chart (Fig. 1G), and the efficacy of EC-Foxp1 deletion in vascular ECs of Foxp1^{ECKO} mice was confirmed by Foxp1 immunostaining (Figs. S1A–B), reverse transcription-quantitative polymerase chain reaction (RT-qPCR) (Fig. S1C) and Western blot (Fig. S1D). Foxp1^{ECKO} mice exhibited a significant increase of tumor growth (Fig. 1H), and final tumor size and mass (Fig. 1I–J) compared to the littermate control mice, with no significant change of mouse body weight (Fig. S1E). A significant increase of blood vessel density in tumors was observed (Fig. 1K–L) and co-staining of Ki-67 and VE-cadherin showed a significantly elevated EC proliferation in LLC1 xenograft tumors (Fig. 1M–N). Similarly elevated tumor angiogenesis and tumor growth were observed in the B16 xenograft tumor model upon EC-Foxp1 deletion (Figs. S2A–H). These results demonstrate that EC-Foxp1 deletion increases xenograft tumor angiogenesis and promotes tumor growth.

2.2. Loss of EC-Foxp1 promotes retinal angiogenesis and exerts in vitro and ex vivo proangiogenic effects during hypoxia condition

As described above, EC-Foxp1 deletion mice had a significant increase of xenograft tumor angiogenesis that promoted the tumor growth. The result is in contrast to a previous study which reported that EC-Foxp1 stimulates angiogenesis [13]. We used a well-established *in vivo* retinal developmental angiogenesis mouse model and the schematic chart of tamoxifen administration for EC-Foxp1 deletion in the retinal angiogenesis model was shown in Fig. 2A. Consistent with previous study, we observed a significant decrease of retinal vessel outgrowth length (Fig. 2B and C) and branching points (Fig. 2B–D) in Foxp1^{ECKO} mice compared to the littermate wild-type control mice under normoxia condition. However, Foxp1^{ECKO} mice exhibited the opposite effects, with a marked increase of retinal vessel outgrowth length and branching points (Fig. 2B–D) under hypoxia condition, which is consistent with our findings in the xenograft tumor angiogenesis model. These results indicate that EC-Foxp1 exerts different angiogenic effects under normoxia and hypoxia conditions, and a significant proangiogenic effect of EC-Foxp1 deletion under hypoxia condition, such as in tumors, possibly results in tumor growth.

Next, we examined whether EC-Foxp1 exerts similar opposite angiogenic activities under normoxia and hypoxia conditions *in vitro* and *ex vivo*. A HUVEC stable cell line carrying lentiviral Foxp1-siRNA was generated and a significant reduction of Foxp1 expression was confirmed in Foxp1 knockdown HUVECs compared to control lentiviral scramble-siRNA HUVECs (Figs. S3A–C). A fibrin gel bead-based sprouting assay showed reduced formation of tip cell sprouts and reduced scattered cell numbers in Foxp1-siRNA knockdown HUVECs compared to those of control scramble-siRNA under normoxia condition (Fig. 2E–G). Conversely, we observed an increased formation of sprouts and elevated scattered cell numbers in Foxp1-siRNA knockdown HUVECs under hypoxia condition (Fig. 2E–G). Similar increased *ex vivo* angiogenic sprouts of aortic ring explants under hypoxia condition were observed from Foxp1^{ECKO} mice compared to littermate wild-type control mice (Fig. 2H–I). These results confirm a significant increase of proangiogenic activity under hypoxia condition in *in vitro* and *ex vivo* angiogenesis models upon EC-Foxp1 deletion.

Endothelial proliferation and migration of ECs are important for sprout angiogenesis. Our studies confirmed the significant increase of EC proliferation under hypoxia in Foxp1 knockdown HUVECs, as shown by Ki67 staining (Figs. S3D–E), cell count (Fig. S3F) and MTT assay (Fig. S3G), as an increase of cell migration by Boyden chamber assay (Figs. S3H–I) and scratch wound-healing assay (Figs. S3J–K), while we used cleaved caspase-3 Western blot, annexin FACs analysis and Caspase 3 immunostainings to confirm that Foxp1 knockdown HUVECs did not influence the death signals (Figs. S4A–E). These results suggest that the increase of angiogenesis upon EC-Foxp1 knockdown under hypoxia is due to an increase of EC proliferation and migration, not due to apoptosis.

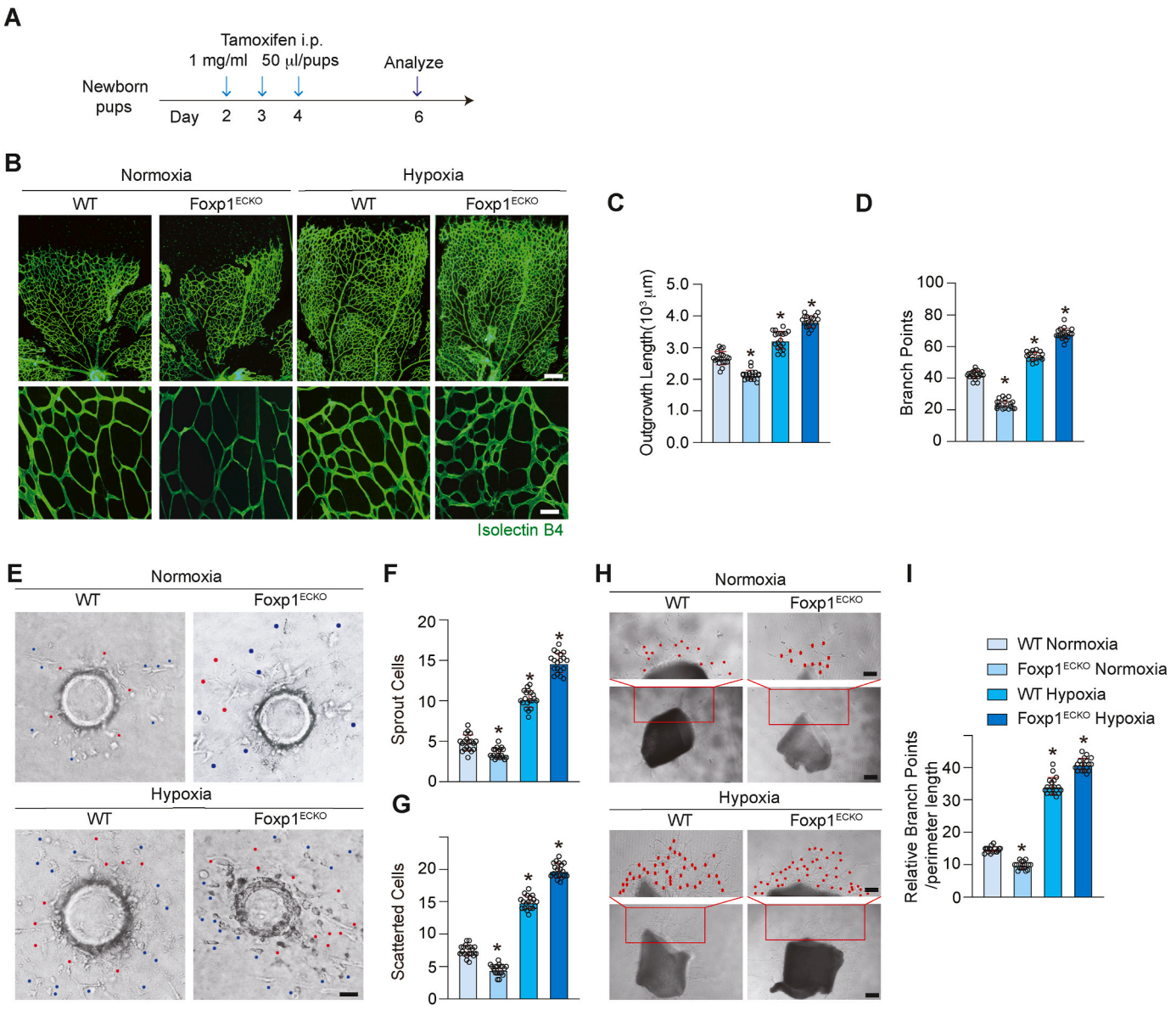

Fig. 2. Sprouting angiogenesis is reduced under normoxia and increased under hypoxia following endothelial Foxp1 deletion. (A) A schematic chart of tamoxifen administration for EC-Foxp1 deletion in mouse retinal angiogenesis model. (B–D) The representative image of retinal sprouting angiogenesis in Foxp1^{ECKO} mutant and wild-type mice under normoxia and hypoxia condition by whole-mount IB4 staining of P6 mouse retina indicated (B), with quantification data of retinal outgrowth length (C) and branch points (D). (E–G) Fibrin gel bead-based *in vitro* sprouting assay, measured by tip cell sprouts and scattered cell numbers, in Foxp1-siRNA knockdown or scramble-siRNA control HUVECs under normoxic and hypoxic condition, with representative image (E) and quantification data (F and G). (H–I) The angiogenic sprouts of *ex vivo* aortic ring explants, measured by branch points, from Foxp1^{ECKO} mutant and wild-type mice under normoxia and hypoxia condition, with representative image (H) and quantification data (I). All data were presented as mean ± SEM, and analyzed using and 2-way ANOVA with Turkey post-hoc test. *, $P < 0.05$; **, $P < 0.01$. Fig. 2C–D quantitative data in accordance with normal distribution. Scale bars: B, 500 μm, 100 μm; E, 100 μm; H, 30 μm; 100 μm.

2.3. EC-Foxp1 gain-of-function represses Hif1α-Hk2 pathway to normalize the hyperglycolysis of tumor ECs and restrict the pro-angiogenic effects and impair tumor growth

Contrary to EC-Foxp1 loss-of-function mice, EC-Foxp1 gain-of-function mice, Foxp1^{ECTg}, exhibited significantly reduced tumor growth (Fig. 3A) and final tumor size and mass (Fig. 3B–C), with a significant reduction of blood vessel density (Fig. 3D–E) in LLC1 xenograft tumor compared to the littermate control mice. Increased expression of Foxp1, but reduced expression of Hif1α and Hk2, was confirmed by RT-qPCR and Western blot in LLC1 xenograft tumor ECs of Foxp1^{ECTg} mice (Fig. 3F–G). Moreover, a significantly reduced retinal angiogenic growth during hypoxia as shown by reduced outgrowth (Fig. 3H and I) and branching points (Fig. 6H–J), was observed in Foxp1^{ECTg} mice compared to the littermate control mice. Similar pro-angiogenic suppression of xenograft tumor vessels and impairment of tumor growth through the Hif1α-Hk2 signal pathway were also observed in B16 xenograft tumor model upon EC-Foxp1 gain-of-function (Figs. S5A–K). These results indicate that EC-Foxp1 gain-of-function protects against tumor growth through inhibition of the EC-Foxp1 dependent Hif1α-Hk2 pathway to normalize the hyperglycolysis in tumor ECs and restrict the pro-angiogenic effects in tumor vessels, suggesting a potential therapeutic value of Hif1α-Hk2 pathway inhibition as anti-angiogenic agents for tumor growth suppression. Finally, the mouse survival time in the xenograft tumor model was examined and a significantly reduced survival time was observed in EC-Foxp1 deletion mice (Figs. S6A–B), with a significantly prolonged time in EC-Foxp1 gain-of-function mice (Figs. S6C–D).

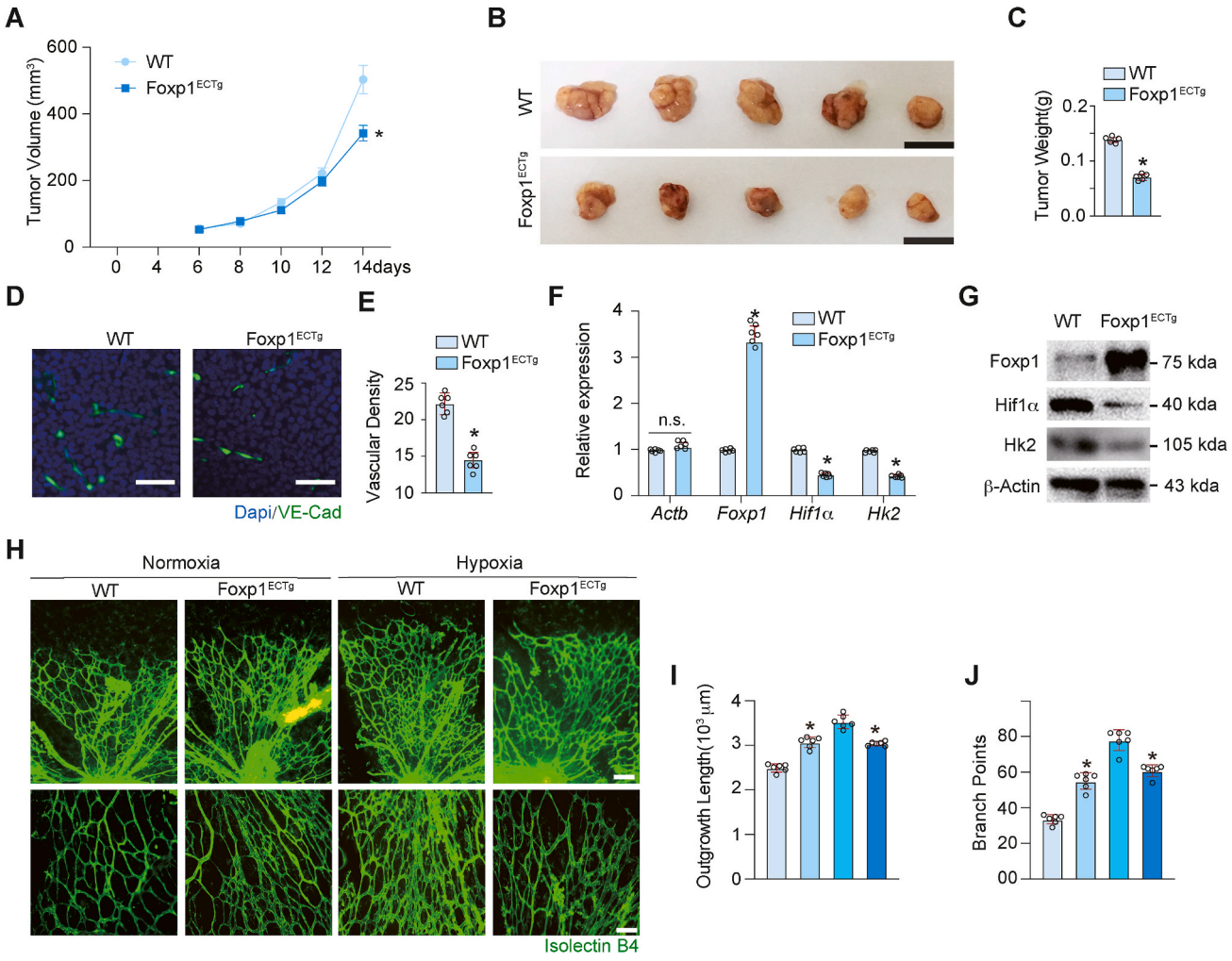

Fig. 3. EC-Foxp1 gain-of-function represses Hif1α-Hk2 signal pathway to restrict the pro-angiogenic effects of tumor ECs and impair tumor growth. (A–E) The tumor growth (A), final tumor size (B), tumor mass (C) and tumor vessel density (D–E) in EC-Foxp1 gain-of-function Foxp1^{ECTg} mutant and littermate wild-type control mice. (F–G) The expression of Hif1α and Hk2 in ECs of Foxp1^{ECTg} mutant and wild-type mice by RT-qPCR (F) and Western blot (G). (H–J) The representative images of retinal angiogenesis in Foxp1^{ECTg} mutant and wild-type mice, with quantification of retinal outgrowth (I) and branch points (J). All data were presented as mean ± SEM, and analyzed using standard two-tailed Student's t-test. *, $P < 0.05$; **, $P < 0.01$. Scale bars: B, 10 mm; D, 50 μm; H, top, 500 μm, bottom, 100 μm.

2.4. HIF1α is identified as a Foxp1 direct downstream target gene under hypoxia and CDKN1A is identified as a FOXP1 direct downstream target gene under normoxia for the regulation of angiogenesis in different oxygen conditions

The tumor vasculature is disordered both structurally and functionally and ECs that comprise the tumor vasculature are poorly connected causing vessel leakage and exposing the endothelium to a hypoxic microenvironment. The transcription factor hypoxia-inducible factor 1α (Hif1α) recently has been implicated in the regulation of many genes responsible for EC metabolism that further regulates angiogenesis [20,21]. To gain insight into the underlying molecular mechanisms of the increased angiogenesis in tumor and developmental retina under hypoxia condition upon EC-Foxp1 deletion, we searched ENDCODE and GEO datasets with keywords Foxp1 Chromatin immunoprecipitation sequence (ChIP-seq) to look for the direct target gene of FOXP1. Analysis of IGV software downloaded wg data files in HUVEC and HepG2 with human hg19 as a reference baseline showed that FOXP1 signal accumulation peaks in *HIF1α* promoter region (Fig. 4A), suggesting *HIF1α* as a possible direct downstream target gene of FOXP1. Sequence analysis found many FOXP1 binding sites in the promoter region of *HIF1α* (Fig. 4B), *HIF1α* mRNA levels (Fig. S7A) and ChIP-qPCR confirmed the association of FOXP1 with *HIF1α* promoter (Fig. 4C) under hypoxia condition. Luciferase assay demonstrated that Foxp1 expression vector dose dependently repressed the promoter of *HIF1α* containing Foxp1 binding sites in ECs (Fig. 4D). Immunostaining (Fig. 4E) and Western blot (Fig. 4F) of cultured ECs displayed a significant increase of *HIF1α* expression under hypoxia condition upon *FOXP1* knockdown. These results indicate *HIF1α* as a FOXP1 direct downstream target gene in ECs.

HIF1α is unstable in well-oxygenated tissues, but stable in hypoxic conditions, owing to the oxygen-dependent ubiquitin-mediated degradation balance with pVHL ubiquitin E3 ligase for degradation [22] and de-ubiquitinase ubiquitin specific peptidase 20 (USP20) preventing degradation [23]. These data suggest that FOXP1 regulates HIF1α in ECs through both transcription and oxygen-dependent ubiquitin-mediated degradation, which further influences tumor angiogenesis required for tumor growth.

FOXP1 was reported to directly repress cell cycle inhibitors p21^{-CIP1} (Cdkn1a) and p27^{-KIP1} and regulate leukemic cell growth [24,25]. We confirmed a significant increase of *CDKN1A* expression upon FOXP1 deletion in ECs (Fig. 4F). Sequence analysis found many FOXP1 binding sites in the promoter region of *CDKN1A* gene (Fig. S7B), ChIP-qPCR confirmed an association of FOXP1 with *CDKN1A* promoter (Fig. S7C), and luciferase assay confirmed that FOXP1 expression vector dose dependently repressed the promoter of *CDKN1A* containing FOXP1 binding sites (Fig. S7D). Further immunostaining showed that FOXP1

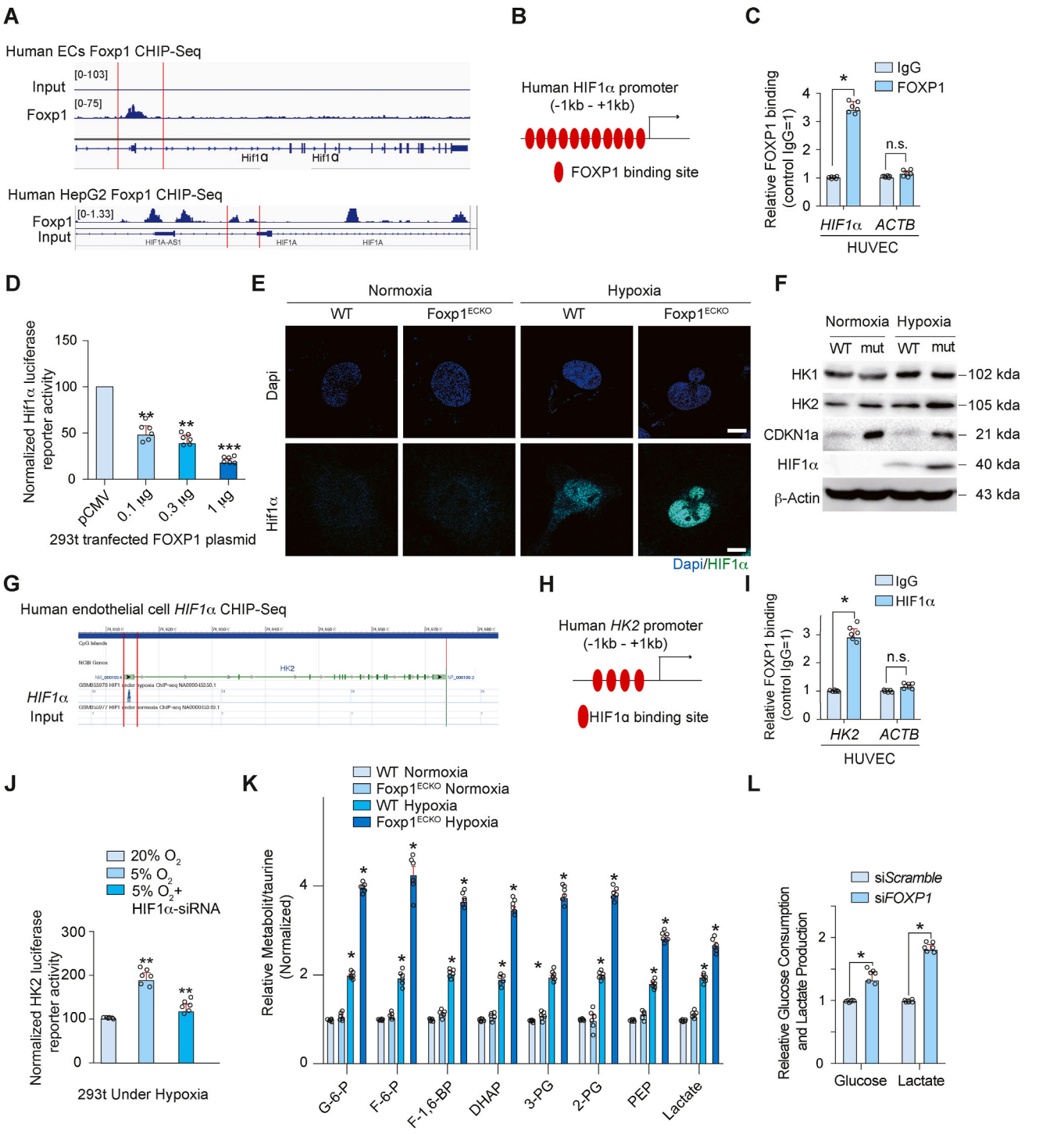

Fig. 4. Hif1α is identified as a Foxp1 direct target gene under hypoxia and Cdkn1a under normoxia and Hif1α further regulates Hk2 controlling EC glycolysis. (A) Analysis of FOXP1 signal accumulation peaks in HIF1α promoter region in mining FOXP1 ChIP-sequence database of HUVEC and HepG2 cell line. (B) Sequence analysis of FOXP1 binding sites at HIF1α promoter region. (C) ChIP-qPCR of FOXP1 and HIF1α promoter. (D) The luciferase activity of the proximal-1kb Hif1α promoter containing Foxp1 binding sites by Foxp1 expression vector. (E) Immunostaining of Hif1α in Foxp1^{ECKO} mutant and wild-type mice. (F) HK1, HK2, P21 (CDKN1A) and HIF1α expression by Western blot in Foxp1^{ECKO} mutant and wild-type mice under normoxic and hypoxic condition. (G) Analysis of Hif1α signal accumulation peaks in Hk2 promoter region in mining Hif1α ChIP-sequence database of HUVECs. (H) Sequence analysis of HIF1α binding sites at HK2 promoter region. (I) ChIP-qPCR of HIF1α and HK2 promoter. (J) The luciferase activity of the proximal-1kb Hk2 promoter containing Hif1α binding sites by hypoxia and Hif1α-siRNA knockdown. (K) Measurement of glycolytic intermediates and lactate in tumor ECs of Foxp1^{ECKO} mutant and wild-type mice under normoxic and hypoxic condition by sigma assay kits, and the intermediates including glucose-6-phosphate (G-6-P), fructose-6-phosphate (F-6-P), Fructose 1, 6-bisphosphatase (F-1, 6-BP), 2-phosphoglycerate (2-PG), 3-phosphoglycerate (3-PG), Dihydroxyacetone phosphate (DHAP) and Phosphoenolpyruvate (PEP) Colorimetric/Fluorometric. (L) The glucose consumption and lactate production of Foxp1 knockdown and scramble-siRNA HUVECs under hypoxia condition. All data were presented as mean ± SEM, and analyzed using standard two-tailed Student's t-test (C, I, L), 1-way ANOVA with Turkey post-hoc test (D, J) and 2-way ANOVA with Turkey post-hoc test (K). *, $P < 0.05$; **, $P < 0.01$. Scale bars: E, 5 μm.

deletion increased *CDKN1A* expression in ECs under normoxia and hypoxia conditions (Figs. S7E–F).

Taken together, these results demonstrate that EC-Foxp1 deletion could restrict angiogenesis under normoxia but promote angiogenesis under hypoxia condition through the regulation of different target genes with *HIF1α* during hypoxia and *CDKN1A* during normoxia.

2.5. FOXP1 targeting hypoxia gene HIF1α regulates HK2 for cell glycolysis metabolism to govern EC phenotype

Recent EC metabolism studies reveal that glycolysis regulators can drive vessel sprouting in parallel to the well-established growth factor-based (genetic) signaling [26,27], as FGF regulation of glycolysis rate-limiting enzyme hexokinase 2 (HK2) is important in EC proliferation and migration for vascular development [28]. HIF1α contains a unique transactivation domain that allows preferential activation of hypoxia-responsive glycolytic genes affecting glycolysis metabolism [29]. We next searched ENDCODE and GEO datasets with keywords HIF1α ChIP-sequence in HUVECs looking for HIF1α target genes as described above. Significant HIF1α signal accumulation peaks in the promoter region of *HK2* in HUVECs (Fig. 4G), and sequence analysis found many HIF1α binding sites in the promoter region of *HK2* (Fig. 4H), suggesting a possible direct regulation of *HK2* by HIF1α for glycolysis metabolism in ECs. ChIP-qPCR indicated an association of HIF1α with *HK2* promoter (Fig. 4I) under hypoxia condition, and luciferase assay showed that the proximal-1kb *HK2* promoter containing HIF1α binding sites was stimulated by decreased oxygen concentration and a significant reversal upon *HIF1α*-siRNA knockdown (Fig. 4J). To define the regulatory role of Foxp1-Hif1α-Hk2 pathway in EC glycolysis, we analyzed the expression of HKs by Western blot. EC-Foxp1 deletion led to a significant increase in HK2 especially under hypoxia, with minimal expression changes of HK1 (Fig. 4F). Examination of the steady-state levels of glycolytic metabolites including Glucose-6-Phosphate (G-6-P), Fructose-6-Phosphate (F-6-P), Fructose 1, 6-bisphosphatase (F-1, 6-BP), 3-Phosphoglycerate (3-PG), 2-Phosphoglycerate (2-PG), Dihydroxyacetone phosphate (DHAP), Phosphoenolpyruvate (PEP) and lactate demonstrated a robust increase in Foxp1^{ECKO} mice under hypoxia compared to wild-type mice (Fig. 4K), which was further confirmed by a significant increase of glucose consumption and lactate production in Foxp1 knockdown HUVECs under hypoxia (Fig. 4L). Further, we examined the products of the pentose phosphate pathway and found that NADPH was significantly increased in the Foxp1 knockout group (Fig. S7G). These results demonstrate that the Foxp1-Hif1α-Hk2 pathway regulated ECs glycolysis metabolism alters ECs phenotype for the regulation of its angiogenic activity.

2.6. EC-Hif1α deletion reverses the EC-Foxp1 deletion mediated hyperglycolysis of tumor ECs and restricts angiogenesis for tumor growth

To define the regulatory step involved in Foxp1-dependent control of Hif1α for glycolysis metabolism in ECs for angiogenic activity, we generated EC-Foxp1 and EC-Hif1α double knockout mice, *Foxp1*^{ECKO}*; Hif1α*^{ECKO}. The tamoxifen administration for EC deletion of Foxp1 and Hif1α was shown in the schematic chart (Fig. 5A) and high efficacy of Hif1α deletion in vascular ECs of *Hif1α*^{ECKO} mutant mice was confirmed (Fig. 5B–C). EC-Hif1α deletion significantly reversed the EC-Foxp1 deletion mediated increase of tumor growth (Fig. 5D), the final tumor size and mass (Fig. 5E–F) compared to the littermate control mice. Immunostaining revealed a significant reversal of elevated blood vessel density (Fig. 5G–H), that was consistent with the increased EC proliferation as evidenced by co-staining of Ki-67 and VE-cadherin in LLC1 xenograft tumors (Fig. 5I–J). Further analysis of the steady-state levels of glycolytic metabolites and lactate in xenograft tumor ECs of *Foxp1*^{ECKO}*;Hif1α*^{ECKO} mice confirmed the EC-Hif1α deletion reversal of tumor EC hyperglycolysis (Fig. 5K), which was further confirmed by glucose consumption and lactate production experiment (Fig. 5L). Moreover, we observed a similar reversal of EC-Hif1α knockdown for EC-Foxp1 deletion mediated increase of angiogenic sprouts in *ex vivo* aortic ring explants under hypoxia condition (Fig. 5M–N). These results demonstrate that the EC-Foxp1-Hif1α-Hk2 pathway regulates the glycolytic metabolism to control EC phenotype impacting tumor angiogenesis and in turn tumor growth.

2.7. RGD-peptide magnetic nanoparticle target delivery of Hif1α-siRNA or Hk2-siRNA into tumor ECs normalizes their hyperglycolysis and restricts angiogenesis for tumor growth suppression

EC-Foxp1 deletion increased Hif1α expression in vascular ECs of LLC1 xenograft tumors to enhance tumor angiogenesis and promote tumor growth. We constructed RGD (Arg-Gly-Asp) peptide–containing magnetic (Fe_3O_4) nanoparticles packaging siRNAs to achieve target delivery of *Hif1α*-siRNA or *Hk2*-siRNA into tumor microvasculature for specific blockade of EC-Hif1α-Hk2 signal pathways [19] in order to determine the effects of Hif1α or Hk2 on tumor angiogenesis and further tumor growth upon EC-Foxp1 deletion. RGD-nanoparticles were injected by the tail vein as shown in Fig. S8A, and the RGD peptide magnetic nanoparticles entered tumor ECs specifically compared to the non-RGD nanoparticles (Figs. S8B–C). A significant reduction of Hif1α (Figs. S7D–E) or Hk2 (Figs. S7F–G) expression was confirmed in vascular ECs of LLC1 xenograft tumors following injection of the nanoparticles. *Hif1α*-siRNA knockdown by RGD-nanoparticles significantly reversed the increased tumor growth (Fig. 6A), final tumor size (Fig. 6B) and tumor mass (Fig. 6C) upon EC-Foxp1 deletion, as well as producing a significant reversal of the elevated blood vessel density in LLC1 xenograft tumor (Fig. 6E–F) in comparison with nanoparticles packing with control scramble siRNA. Measurement of glycolytic metabolites and lactate in xenograft tumor ECs demonstrated a significant normalization of the metabolites in EC-Foxp1 deletion mice following injection of nanoparticles packed with *Hif1α*-siRNA (Fig. 6D). Similarly, nanoparticles of *Hk2*-siRNA knockdown significantly suppressed the tumor growth (Fig. 6G–I) through normalization of the elevation of glycolytic metabolites (Fig. 6J), reversal of increased glucose consumption and lactate production (Fig. 6M–N) that restricted the EC-Foxp1 deletion mediated increase of xenograft tumor angiogenesis (Fig. 6K–L). Moreover, knockdown of Hif1α (Figs. S9A–I) or Hk2 (Figs. S10A–I) expression in EC-Foxp1 deletion mice by RGD-nanoparticles exerted the similar reversal of elevated glycolytic metabolites, further reversal of the increased tumor vessel density, and finally suppression of tumor growth in B16 xenograft tumor model (Figs. S9–10).

However, no significant alteration of tumor angiogenesis and tumor growth was observed in EC-Foxp1 deletion mice following EC target delivery of nanoparticles packaging with *Cdkn1a (p21)*-siRNA, the Foxp1 target gene under normoxic condition (Fig. 6A–F). Measurement of glycolytic metabolites and lactate in tumor ECs confirmed no alteration in EC-Foxp1 deletion mice by *Cdkn1a*-siRNA nanoparticles (Fig. 6D). Finally, we used the retinal developmental angiogenesis model demonstrating that the nanoparticles carrying *Cdkn1a*-siRNA significantly reversed the elevated retinal vessel outgrowth length upon EC-Foxp1 deletion under normoxic condition, with no significant alteration under hypoxic condition (Fig. 6O–Q), suggesting that EC-Foxp1 regulation of the Hif1α-Hk2 signal pathway might be more important in the regulation of tumor ECs metabolism for angiogenic activity responsible for tumor growth that is under hypoxia condition.

Consistent with the *in vivo* findings, inhibition of Hif1α or Hk2 expression by RGD-nanoparticles packaging *Hif1α*-siRNA or *Hk2*-siRNA significantly reversed the elevated angiogenic sprouting in *ex vivo* aortic ring explants of EC-Foxp1 deletion mice (Figs. S11A–B), and *in vitro* angiogenic sprouting in cultured ECs by fibrin gel bead-based sprouting assay upon Foxp1-siRNA knockdown under hypoxia (Figs. S11C–D). A similar reversal of the elevated cell proliferation and migration by RGD-nanoparticles packaging *Hif1α*-siRNA or *HK2*-siRNA was observed in *in vitro* cultured ECs upon *Foxp1*-siRNA knockdown under hypoxia

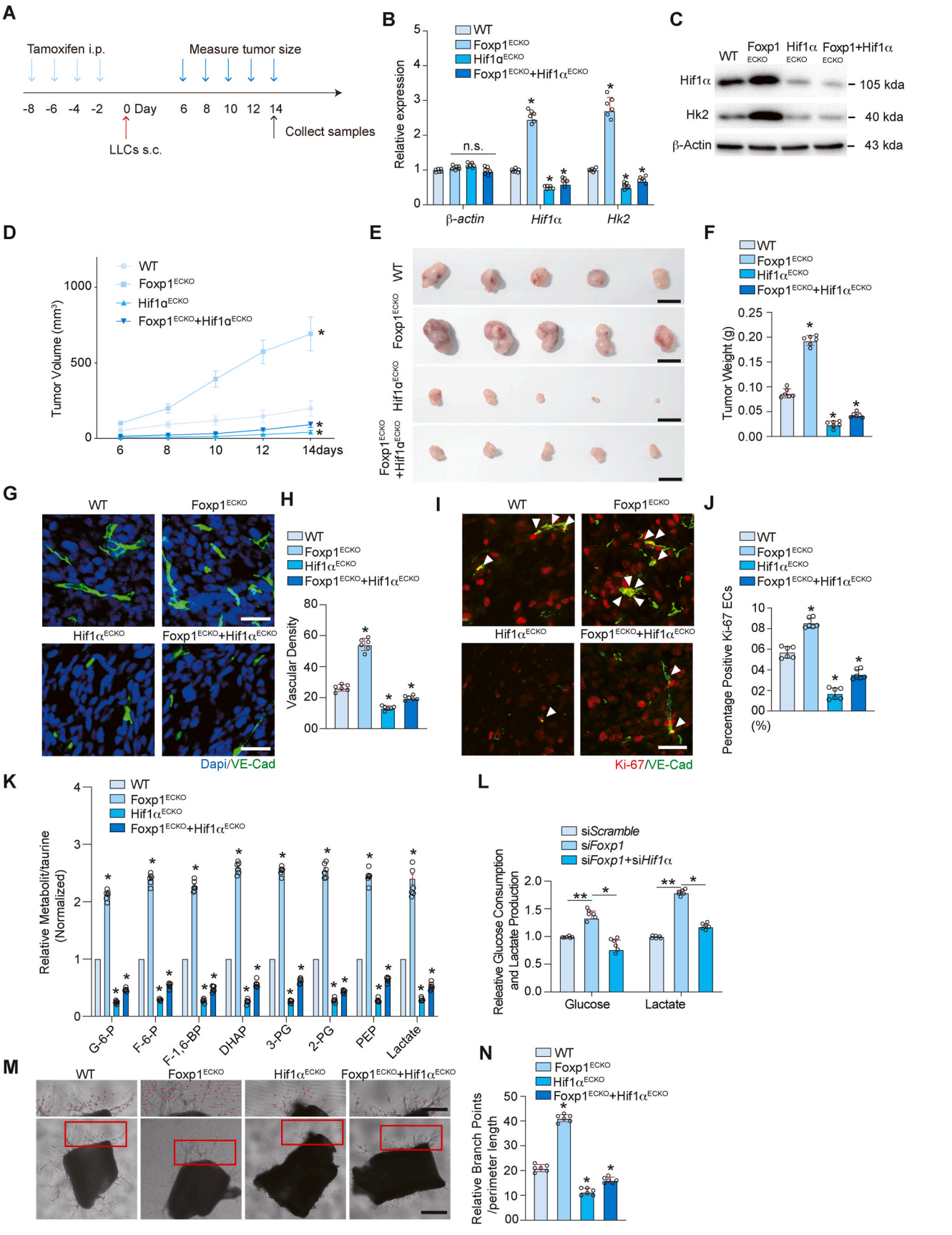

(caption on next page)

Fig. 5. EC-Hif1α deletion reverses the EC-Foxp1 deletion mediated elevation of EC hyperglycolysis and restricts tumor angiogenesis for tumor growth suppression. (A) The schematic chart of tamoxifen administration for induction of EC-Foxp1 and EC-Hif1α deletion in $Foxp1^{ECKO}$;$Hif1α^{ECKO}$ double knockout mice for LLC1 xenograft tumor model. (B–C) The expression of Hif1α, Hk2 and p21 in ECs of $Foxp1^{ECKO}$;$Hif1α^{ECKO}$, $Hif1α^{ECKO}$, $Foxp1^{ECKO}$ and littermate wild-type mice by RT-qPCR (B) and Western blot (C). (D–F) The tumor growth (D), final tumor size (E) and tumor mass (F) in $Foxp1^{ECKO}$;$Hif1α^{ECKO}$, $Hif1α^{ECKO}$, $Foxp1^{ECKO}$ and littermate wild-type mice. (G–H) The representative images of vessel density (G–H) and co-staining of Ki67 indicated by white arrow heads and VE-cadherin (I–J) in xenograft tumor sections of $Foxp1^{ECKO}$;$Hif1α^{ECKO}$, $Hif1α^{ECKO}$, $Foxp1^{ECKO}$ and littermate wild-type mice, with quantification data on the right. (K) The measurement of glycolytic intermediates and lactate in tumor ECs of $Foxp1^{ECKO}$;$Hif1α^{ECKO}$, $Hif1α^{ECKO}$, $Foxp1^{ECKO}$ and littermate wild-type mice. (L) The glucose consumption and lactate production in Foxp1/Hif1α, Hif1α, Foxp1 knockdown and scramble-siRNA control HUVECs. (M–N) The representative images of angiogenic sprouts of *ex vivo* aortic ring explants from $Foxp1^{ECKO}$;$Hif1α^{ECKO}$, $Hif1α^{ECKO}$, $Foxp1^{ECKO}$ and littermate wild-type mice, with quantification data on the right. All data were presented as mean ± SEM, and analyzed using 2-way ANOVA with Turkey post-hoc test (B, D, F, H, J and K) and 1-way ANOVA with Turkey post-hoc test (N). *, $P < 0.05$; **, $P < 0.01$. Scale bars: E, 10 mm; G, I, 50 μm; M, 30 μm, 100 μm.

compared to the control scramble siRNA, shown by cell proliferation assay of Ki-67 staining (Figs. S11E–F), cell count (Fig. S11G) and MTT assay (Fig. S11H), and cell migration assay of Boyden chamber assay (Figs. S11I–J), respectively.

Taken together, these *in vivo* and *in vitro* results demonstrate that EC-Foxp1 regulates different signal pathways for angiogenic activity under hypoxia or normoxia conditions, with Foxp1 deletion mediated elevation of Hif1α-Hk2 pathway leading to EC hyperglycolysis, the microenvironment that tumor vasculature has, to promote angiogenesis required for tumor growth.

3. Discussion

In this study, database mining shows a reduced Foxp1 expression in lung carcinoma LUSC and LUAD and a correlation of Foxp1 expression level with the survival time of carcinoma patients was observed. We confirm that Foxp1 expression is mainly reduced in tumor ECs, and that EC-Foxp1 deletion exerts pro-angiogenic effects and promotes tumor growth. Hif1α and in turn Hk2 are identified as Foxp1 downstream target genes in ECs to regulate glycolytic metabolism for cell proliferation and migration without alteration of apoptosis, which is in line with the repression of tumor vessel overgrowth to impair tumor growth (Fig. 7).

ECs form the inner lining of blood vessels and are highly plastic cells. ECs stay mostly quiescent and become active to switch rapidly into a highly migratory and proliferative state during vessel sprouting in response to tissue damage or as a result of pathological conditions such as inflammation, cancer and diabetes. This angiogenic switch has long been considered to be dictated by angiogenic growth factors and other signals, e.g. Notch and cell cycle regulation as Cdkn1a, $p21^{-CIP1}$ cell cycle inhibitor [30,31]. Foxp1, a member of the FOX family of transcription factors, has a broad range of functions, and could act as a repressor of Cdkn1a and retinoblastoma protein (Rb) transcription to directly interact with the tumor suppressor p53 and inhibit its activity and drive osteosarcoma development [32]. Also, Foxp1 repressed the expression of the $p21^{-CIP1}$ and $p27^{-KIP1}$ cell cycle inhibitors to drive expansion of hematopoietic stem/progenitor and leukemia cells [25]. Our previous study indicated that endocardium Foxp1 regulated the Sox17-β-catenin-FGFs pathway to control cardiomyocyte proliferation for heart development [33]. In the current study, we identified Cdkn1a as a Foxp1 direct target gene and EC-Foxp1 deletion increased p21 expression in ECs to restrict the retinal angiogenesis under normoxia (Fig. 7). However, a significantly enhanced retinal angiogenesis was observed under hypoxia, indicating other pathways might be involved in the regulation of angiogenesis under hypoxic condition.

Recent studies reveal that glycolysis is the main energy source in the endothelium with sprouting ECs having higher glycolysis rates in the same range as many cancer cells, and the growth factors and transcriptional signals converge on metabolic changes that drive vessel sprouting [26,27]. VEGF-stimulated ECs doubled their glycolytic flux through activation of PFKFB3, the second rate-limiting glycolysis enzyme, to meet increased overall energy demands during EC proliferation and migration [26,34], and FGF-dependent regulation of HK2 endothelial glycolysis is crucial in developmental and adult vascular growth [28], while flow-responsive transcription factor KL2 binds to the PFKFB3 promoter to subsequently repress PFKFB3 transcription which decreases sprouting capacity, vessel branching and outgrowth [35].

Tumor ECs rewire their central metabolism when becoming dysfunctional and during pathological vessel overgrowth, and this obvious connection between metabolic maladaptation and dysfunction in tumor ECs calls for deeper understanding of the most detailed features of EC metabolism to advance translation into therapeutics. We found reduced Foxp1 in ECs of human lung carcinoma and LLC1 xenograft tumors, and identified EC-Foxp1 regulation of its target gene Hif1α and then Hk2 to govern tumor EC metabolism and function, and thereby control tumor growth.

As angiogenesis is essential for tumor growth and metastasis, controlling tumor-associated angiogenesis is a promising tactic in limiting cancer growth and progression. The blood vessels surrounding the tumor not only provide nutrients, oxygen and metabolites, but also provide a pathway for tumor cells to metastasize. One of the major challenges facing clinical anti-angiogenesis therapy today is how to maximize the therapeutic effect and minimize side effects. Tumor endothelial cells (TECs) are significantly different from normal ECs, which are characterized by genetic instability, genetic heterogeneity, anorexia resistance, metabolic abnormalities, resistance to anticancer drugs, and maladaptive mechanical microenvironments [36]. TECs play an important role in tumor progression and metastasis. There is growing evidence that TECs are promising target than normal ECs [37], and the complexity and intricate details of the tumor microenvironment remain unclear, uniform standard is lacking in detecting TEC. A comprehensive description of the tumor microenvironment and a better understanding of the underlying mechanisms of how TECs form and function will help find novel targets to overcome drug resistance and monitor the effects of anti-angiogenic therapies [38,39]. Therefore, unlike current anti-angiogenic therapies which block a single target and usually fail in clinical use, mostly because of the induction of compensatory mechanisms, targeting TEC metabolism is a more global approach to target key metabolic players without inciting compensatory feedback mechanisms. In this current study, we demonstrated that RGD-nanoparticle target delivery of Hk2-siRNA specifically into TECs could improve the hyperglycolysis induced by upregulation of Hif1α upon EC-Foxp1 deletion and inhibit its pro-angiogenic effects with further tumor growth suppression.

Further, we examined the products of the pentose phosphate pathway and found that NADPH was significantly increased in the Foxp1 knockout group (Fig. S7G). This result demonstrated that the Foxp1-Hif1α-Hk2 pathway may also regulate ECs pentose phosphate metabolism to participate in altering ECs phenotype for the regulation of its angiogenic activity, but how EC-Foxp1-Hif1α-Hk2 pathway participated in regulating pentose phosphate need further investigation.

In conclusion, this study found that EC-Foxp1 regulation of an Hif1α-Hk2 pathway in the endothelium could improve the hyperglycolysis of tumor ECs and restrict tumor angiogenesis, and further potently retard tumor growth, therefore offering a novel strategy to improve anticancer therapy.

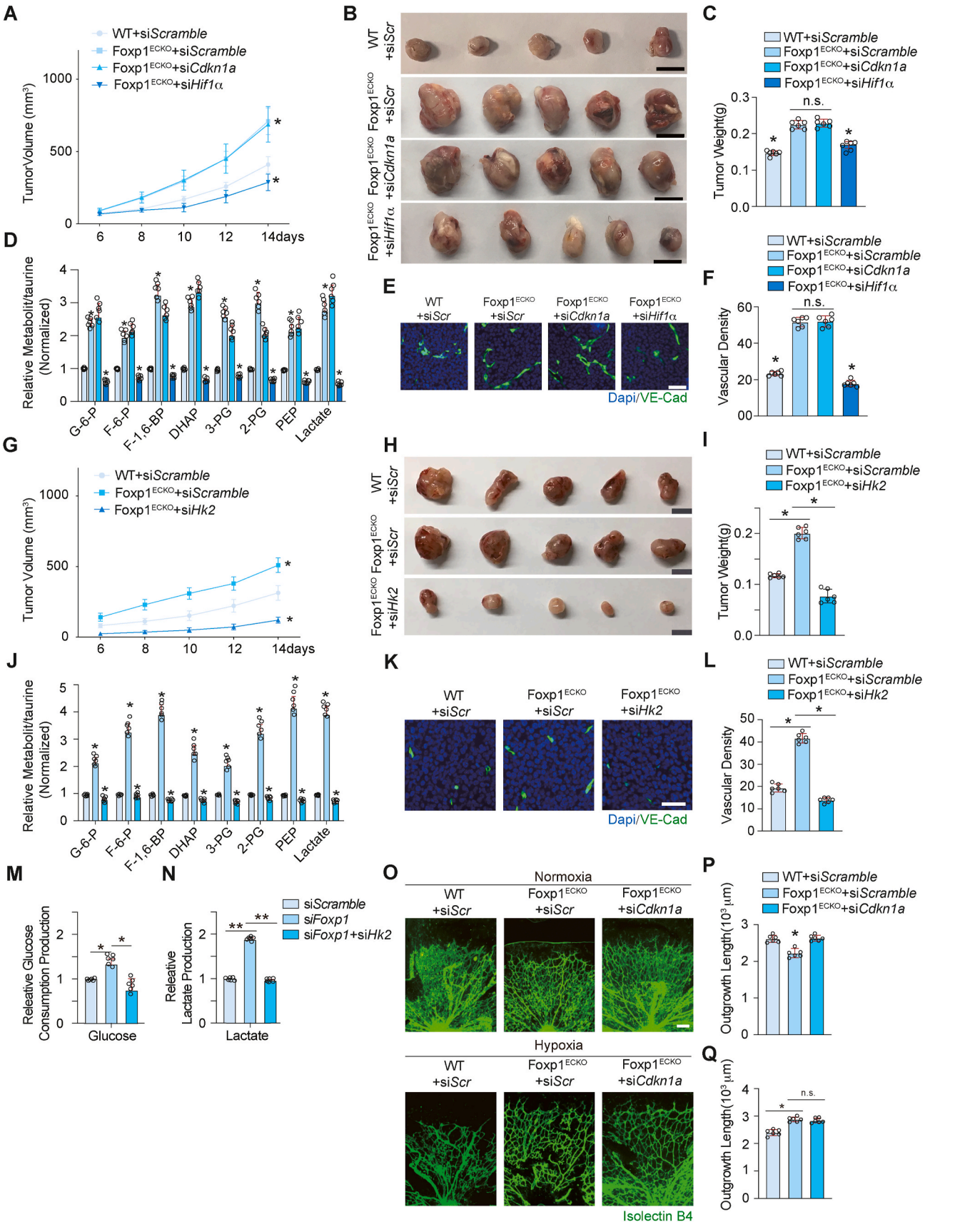

(caption on next page)

Fig. 6. RGD-peptide magnetic nanoparticle target delivery of Hif1α-siRNA or Hk2-siRNA to tumor ECs reduces the hyperglycolysis to restrict tumor angiogenesis and impair tumor growth. (A–C) The tumor growth (A), final tumor size (B) and tumor mass (C) in Foxp1^{ECKO} mice following administration of RGD-peptide magnetic nanoparticles packaging Hif1α-siRNA or P21-siRNA for target delivery of the siRNA to tumor ECs. (D–E) The measurement of glycolytic intermediates and lactate in tumor ECs (D), and the representative images of tumor vessel density (E) with quantification data (F), in Foxp1^{ECKO} mice following administration of RGD-peptide magnetic nanoparticles packaging Hif1α-siRNA or P21-siRNA. (G–J) The tumor growth (G), final tumor size (H), tumor mass (I) and the measurement of glycolytic intermediates and lactate of tumor ECs (J) in Foxp1^{ECKO} mice following administration of RGD-peptide magnetic nanoparticles packaging Hk2-siRNA. (K) The glucose consumption and lactate production in Hk2-siRNA knockdown and scramble-siRNA control HUVECs. (L–M) The representative images of xenograft tumor vessel density (L) and retinal angiogenesis (M) in Foxp1^{ECKO} mice following administration of RGD-peptide magnetic nanoparticles packaging Hk2-siRNA, with quantification data on the right. All data were presented as mean ± SEM, and analyzed using standard two-tailed Student's t-test (A and C–F) and 2-way ANOVA with Turkey post-hoc test (J, O). *, $P < 0.05$; **, $P < 0.01$. Scale bars: B, H 10 mm; K, O, 50 μm; M, 500 μm.

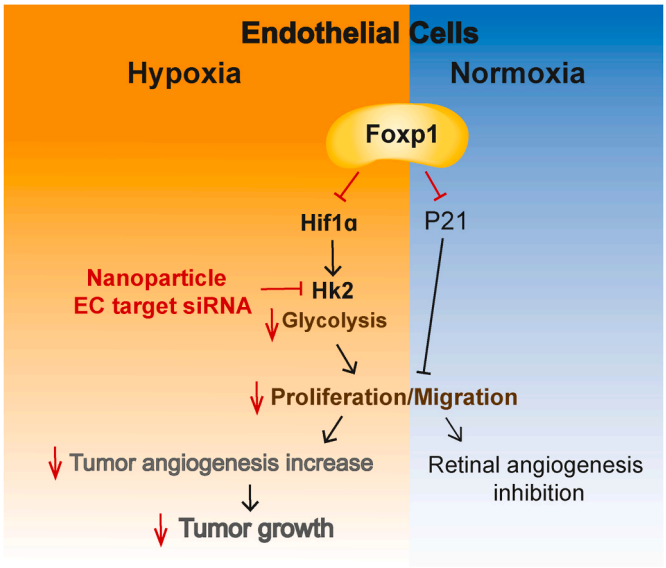

Fig. 7. Model of how endothelial Foxp1 regulates EC phenotypes under hypoxia and normoxia condition by targeting different pathways. EC-Foxp1 represses Hif1α and in turn Hk2 expression to improve hyperglycolysis of tumors ECs and reduces cell proliferation and migration, and thus exert anti-angiogenic effects for tumor growth suppression.

4. Materials and methods

Detailed experimental procedures, mice and human lung squamous cell carcinoma (LUSC) microarray tissue samples are described in online materials and methods and all are available within the article and its online supplementary files.

CRediT authorship contribution statement

Jingjiang Pi: Data curation, Conceptualization. **Jie Liu:** Methodology, Data curation. **Huan Chang:** Software, Data curation. **Xiaoli Chen:** Validation, Formal analysis. **Wenqi Pan:** Data curation. **Qi Zhang:** Validation, Supervision, Funding acquisition. **Tao Zhuang:** Project administration, Methodology, Data curation. **Jiwen Liu:** Software, Data curation. **Haikun Wang:** Validation, Supervision. **Brian Tomlinson:** Writing – review & editing, Writing – original draft. **Paul Chan:** Software, Formal analysis. **Yu Cheng:** Methodology. **Zuoren Yu:** Supervision, Investigation. **Lin Zhang:** Writing – review & editing, Supervision, Funding acquisition. **Zhenlin Zhao:** Visualization, Funding acquisition. **Zhongmin Liu:** Supervision, Funding acquisition. **Jie Liu:** Writing – review & editing, Methodology, Conceptualization. **Yuzhen Zhang:** Writing – review & editing, Supervision, Conceptualization.

Declaration of competing interest

There are no competing interests.

Data availability

Data will be made available on request.

Acknowledgments

This study was supported by funds from the National Key Research and Development Program (2022YFA1104503), National Natural Science Foundation of China (82270432, 81903171, 82130016, 82170477, 82070456, 82270260, 82170257, 82200554), Research Program of Shenzhen Science and Technology Innovation Committee (JCYJ20220530163603008, JCYJ20220530163601003), Natural Science Foundation of Guangdong Province (2023A1515010880), Young Medical Talents Training Program of Health Bureau of Shanghai (2022YQ035), Young Medical Talents Training Program of Pudong Health Bureau of Shanghai (PWRq2021-04), Sino-German Center Mobility Program (M0680), Innovative research team of high-level local universities in Shanghai and a key laboratory program of the Education Commission of Shanghai Municipality (ZDSYS14005), Key Disciplines Group Construction Project of Shanghai Pudong New Area Health Commission (Grant No. PWZxq2022-02, PWZxk2022-20), The Top-level Clinical Discipline Project of Shanghai Pudong (PWYgf2021-01).

Appendix A. Supplementary data

Supplementary data to this article can be found online at https://doi.org/10.1016/j.redox.2024.103281.

References

[1] P. Carmeliet, R.K. Jain, Molecular mechanisms and clinical applications of angiogenesis, Nature 473 (7347) (2011) 298–307.
[2] N. Ferrara, R.S. Kerbel, Angiogenesis as a therapeutic target, Nature 438 (7070) (2005) 967–974.
[3] K. Hida, N. Maishi, D.A. Annan, Y. Hida, Contribution of tumor endothelial cells in cancer progression, Int. J. Mol. Sci. 19 (5) (2018).
[4] G. Bergers, D. Hanahan, Modes of resistance to anti-angiogenic therapy, Nat. Rev. Cancer 8 (8) (2008) 592–603.
[5] G. Eelen, P. de Zeeuw, L. Treps, U. Harjes, B.W. Wong, P. Carmeliet, Endothelial cell metabolism, Physiol. Rev. 98 (1) (2018) 3–58.
[6] F. Lopes-Coelho, F. Martins, J. Serpa, Endothelial cells (ECs) metabolism: a valuable piece to disentangle cancer biology, Adv. Exp. Med. Biol. 1219 (2020) 143–159.
[7] L.N. Groschner, M. Waldeck-Weiermair, R. Malli, W.F. Graier, Endothelial mitochondria–less respiration, more integration, Pflueg. Arch. Eur. J. Physiol. 464 (1) (2012) 63–76.
[8] J.W. Lee, S.H. Bae, J.W. Jeong, S.H. Kim, K.W. Kim, Hypoxia-inducible factor (HIF-1)alpha: its protein stability and biological functions, Exp. Mol. Med. 36 (1) (2004) 1–12.
[9] W. Wei, X.D. Yu, Hypoxia-inducible factors: crosstalk between their protein stability and protein degradation, Cancer Lett. 257 (2) (2007) 145–156.
[10] R. Bartoszewski, A. Moszynska, M. Serocki, A. Cabaj, A. Polten, R. Ochocka, et al., Primary endothelial cell-specific regulation of hypoxia-inducible factor (HIF)-1 and HIF-2 and their target gene expression profiles during hypoxia, Faseb. J. : official publication of the Federation of American Societies for Experimental Biology 33 (7) (2019) 7929–7941.
[11] S. Li, J. Weidenfeld, E.E. Morrisey, Transcriptional and DNA binding activity of the Foxp1/2/4 family is modulated by heterotypic and homotypic protein interactions, Mol. Cell Biol. 24 (2) (2004) 809–822.
[12] W. Shu, M.M. Lu, Y. Zhang, P.W. Tucker, D. Zhou, E.E. Morrisey, Foxp2 and Foxp1 cooperatively regulate lung and esophagus development, Development 134 (10) (2007) 1991–2000.

[13] S. Grundmann, C. Lindmayer, F.P. Hans, I. Hoefer, T. Helbing, G. Pasterkamp, et al., FoxP1 stimulates angiogenesis by repressing the inhibitory guidance protein semaphorin 5B in endothelial cells, PLoS One 8 (9) (2013) e70873.
[14] A.H. Banham, N. Beasley, E. Campo, P.L. Fernandez, C. Fidler, K. Gatter, et al., The FOXP1 winged helix transcription factor is a novel candidate tumor suppressor gene on chromosome 3p, Cancer Res. 61 (24) (2001) 8820–8829.
[15] S.B. Fox, P. Brown, C. Han, S. Ashe, R.D. Leek, A.L. Harris, et al., Expression of the forkhead transcription factor FOXP1 is associated with estrogen receptor alpha and improved survival in primary human breast carcinomas, Clin. Cancer Res. : Offi. J. American Assoc. Cancer Res. 10 (10) (2004) 3521–3527.
[16] H.B. Koon, G.C. Ippolito, A.H. Banham, P.W. Tucker, FOXP1: a potential therapeutic target in cancer, Expert Opin. Ther. Targets 11 (7) (2007) 955–965.
[17] M. Katoh, M. Igarashi, H. Fukuda, H. Nakagama, M. Katoh, Cancer genetics and genomics of human FOX family genes, Cancer Lett. 328 (2) (2013) 198–206.
[18] R. Rad, L. Rad, W. Wang, A. Strong, H. Ponstingl, I.F. Bronner, et al., A conditional piggyBac transposition system for genetic screening in mice identifies oncogenic networks in pancreatic cancer, Nat. Genet. 47 (1) (2015) 47–56.
[19] J. Pi, T. Tao, T. Zhuang, H. Sun, X. Chen, J. Liu, et al., A MicroRNA302-367-erk1/2-klf2-S1pr1 pathway prevents tumor growth via restricting angiogenesis and improving vascular stability, Circ. Res. 120 (1) (2017) 85–98.
[20] C.W. Pugh, P.J. Ratcliffe, Regulation of angiogenesis by hypoxia: role of the HIF system, Nat. Med. 9 (6) (2003) 677–684.
[21] N. Tang, L. Wang, J. Esko, F.J. Giordano, Y. Huang, H.P. Gerber, et al., Loss of HIF-1alpha in endothelial cells disrupts a hypoxia-driven VEGF autocrine loop necessary for tumorigenesis, Cancer Cell 6 (5) (2004) 485–495.
[22] P.H. Maxwell, M.S. Wiesener, G.W. Chang, S.C. Clifford, E.C. Vaux, M.E. Cockman, et al., The tumour suppressor protein VHL targets hypoxia-inducible factors for oxygen-dependent proteolysis, Nature 399 (6733) (1999) 271–275.
[23] Z. Li, D. Wang, E.M. Messing, G. Wu, VHL protein-interacting deubiquitinating enzyme 2 deubiquitinates and stabilizes HIF-1alpha, EMBO Rep. 6 (4) (2005) 373–378.
[24] E.W. Lam, J.J. Brosens, A.R. Gomes, C.Y. Koo, Forkhead box proteins: tuning forks for transcriptional harmony, Nat. Rev. Cancer 13 (7) (2013) 482–495.
[25] C. Naudin, A. Hattabi, F. Michelet, A. Miri-Nezhad, A. Benyoucef, F. Pflumio, et al., PUMILIO/FOXP1 signaling drives expansion of hematopoietic stem/progenitor and leukemia cells, Blood 129 (18) (2017) 2493–2506.
[26] K. De Bock, M. Georgiadou, S. Schoors, A. Kuchnio, B.W. Wong, A.R. Cantelmo, et al., Role of PFKFB3-driven glycolysis in vessel sprouting, Cell 154 (3) (2013) 651–663.
[27] S. Schoors, U. Bruning, R. Missiaen, K.C. Queiroz, G. Borgers, I. Elia, et al., Fatty acid carbon is essential for dNTP synthesis in endothelial cells, Nature 520 (7546) (2015) 192–197.
[28] P. Yu, K. Wilhelm, A. Dubrac, J.K. Tung, T.C. Alves, J.S. Fang, et al., FGF-dependent metabolic control of vascular development, Nature 545 (7653) (2017) 224–228.
[29] C.J. Hu, A. Sataur, L. Wang, H. Chen, M.C. Simon, The N-terminal transactivation domain confers target gene specificity of hypoxia-inducible factors HIF-1alpha and HIF-2alpha, Mol. Biol. Cell 18 (11) (2007) 4528–4542.
[30] R. Brutsch, S.S. Liebler, J. Wustehube, A. Bartol, S.E. Herberich, M.G. Adam, et al., Integrin cytoplasmic domain-associated protein-1 attenuates sprouting angiogenesis, Circ. Res. 107 (5) (2010) 592–601.
[31] S.M. Weis, D.A. Cheresh, Tumor angiogenesis: molecular pathways and therapeutic targets, Nat. Med. 17 (11) (2011) 1359–1370.
[32] H. Li, X. Han, S. Yang, Y. Wang, Y. Dong, T. Tang, FOXP1 drives osteosarcoma development by repressing P21 and RB transcription downstream of P53, Oncogene 40 (15) (2021) 2785–2802.
[33] Y. Zhang, S. Li, L. Yuan, Y. Tian, J. Weidenfeld, J. Yang, et al., Foxp1 coordinates cardiomyocyte proliferation through both cell-autonomous and nonautonomous mechanisms, Gene Dev. 24 (16) (2010) 1746–1757.
[34] S. Schoors, K. De Bock, A.R. Cantelmo, M. Georgiadou, B. Ghesquiere, S. Cauwenberghs, et al., Partial and transient reduction of glycolysis by PFKFB3 blockade reduces pathological angiogenesis, Cell Metabol. 19 (1) (2014) 37–48.
[35] A. Doddaballapur, K.M. Michalik, Y. Manavski, T. Lucas, R.H. Houtkooper, X. You, et al., Laminar shear stress inhibits endothelial cell metabolism via KLF2-mediated repression of PFKFB3, Arterioscler. Thromb. Vasc. Biol. 35 (1) (2015) 137–145.
[36] X. Yao, Y. Zeng, Tumour associated endothelial cells: origin, characteristics and role in metastasis and anti-angiogenic resistance, Front. Physiol. 14 (2023) 1199225.
[37] K. Hida, Y. Hida, D.N. Amin, A.F. Flint, D. Panigrahy, C.C. Morton, et al., Tumor-associated endothelial cells with cytogenetic abnormalities, Cancer Res. 64 (22) (2004) 8249–8255.
[38] J. Goveia, K. Rohlenova, F. Taverna, L. Treps, L.C. Conradi, A. Pircher, et al., An integrated gene expression landscape profiling approach to identify lung tumor endothelial cell heterogeneity and angiogenic candidates, Cancer Cell 37 (3) (2020) 421.
[39] J.M. Butler, H. Kobayashi, S. Rafii, Instructive role of the vascular niche in promoting tumour growth and tissue repair by angiocrine factors, Nat. Rev. Cancer 10 (2) (2010) 138–146.